Lasers in Manufacturing Conference 2019

Fs laser micromachining applied to the manufacturing of glass-based devices

A. Champion[a*], A. Henrottin[a], D. Bruneel[a], J. A. Ramos-de-Campos[a], A. Kupisiewicz[a]

[a]*LASEA S.A., Rue des Chasseurs Ardennais, 10, 4031 Angleur, Belgium*

Abstract

Micromachining of glass using femtosecond laser is used in different fields such as micro-fluidic, smartphone and automotive. The interaction between laser and glass leads to different effects such as volume variation leading to stress, melting and ablation at the focus point. These effects can be controlled with the laser parameters and allow to weld, to make channels and to cut the glass along thin and accurate patterns. In this work we present different applications in glass. At first, glass cutting of plates along curved pattern by controlling cracks propagation. Then channels are engraved on the surface of the glass using ablation process. To finish, welding of channels in glass is studied targeting applications for micro-fluidic devices.

Keywords: Femto Second Laser, Welding, Cutting, Micromachining;

1. Introduction

Femtosecond lasers are widely used to machine transparent material. When the laser interacts with glass, different phenomena occur at the focused point. At first with low energy, the refractive index increases as shown in Canning et al., 2011, Davis et al., 1996, when the energy continues to increase, a positive volume variation creates stress in and around the laser affected zone as described in Champion et al.,2012, Champion et al. 2013. If the energy rises again, ablation or melting takes place. In addition, in transparent material, when a critical power is reached, self-focusing occurs. This phenomenon is called the Kerr-effect and the refractive index is locally increased. When the plasma density increases the beam is defocused. A

* Corresponding author. Tel.: +32-436-502-43;
E-mail address: AChampion@lasea.com .

competition between these phenomena allows to create a filament along the propagation direction as shown in Fibich et al., 2000, Mourou et al., 2006, Couairon et al., 2000.

Cutting of transparent material is used in different field as smartphone in order to cut screens and in automotive. It has been proven that in using beam shaping to elongate the focus point, filamentation and burst instead of a single pulse, cutting is achievable as explained in Kumkar et al., 2014. Amplitude, has developed a module allowing to cut glass by using Bessel beam shaping, and by using oriented cracks according to the cutting direction. This work is described in Mishchik et al., 2017.

In the micro-fluidic field, lab on chips are developed for medical applications and chemical analysis. Up to now these lab-on-chips are fabricated with lithography or other processes that take more time and use chemicals. However, laser technology starts to be studied to weld transparent materials as the Borofloat®. This technology allows to make complex forms due to the accuracy and reduce the cycle time. For instance, in Kongsuwan et al., 2012, welding is performed in using microscope objective to focus the beam. A model of the melted areas is developed according to the residual stress in the welding.

In our work we present glass cutting and glass welding of transparent materials by using the same glass module. At first, filamentation allows to cut the glass along curved trajectories, on flat samples or on tubes. Thanks to the beam shaping, oriented cracks form according to the writing direction. A cleavage is necessary to separate parts. Then, the same system is used to weld channels for microfluidic. Indeed, under higher frequencies, the glass melts along and between filaments, due to the heat accumulation. Therefore, a homogeneous local melting is achieved. Channels are made in digging grooves on the surface of a plate by ablation with a lens combined to a scanner head.

2. Protocol

In the next part, two different uses of burst are described to accumulate energy and achieve longer laser affected zones combined with two optical configurations.

2.1. Setup

A Yuja laser from Amplitude provides a laser beam with a frequency of 100 kHz and a maximum power of 10 W. The laser parameters are controlled with the amplitude software. In the Fig 1 the setup is illustrated.

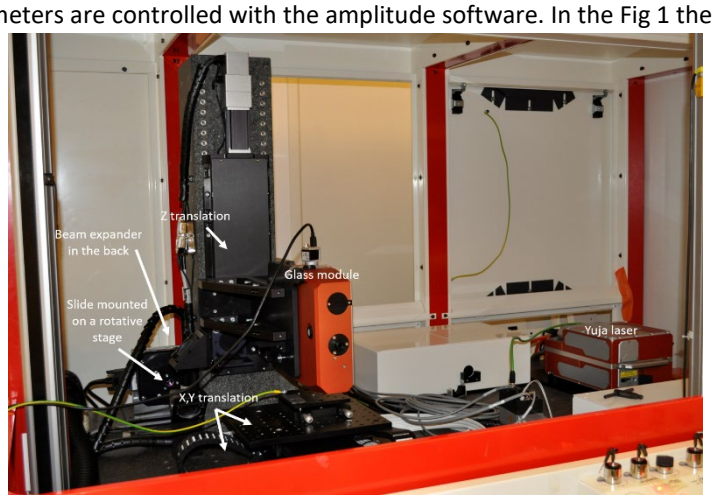

Fig. 1. Setup description.

The beam is focused on the sample using a system called “Module GLASS” from Amplitude as well. This module allows to do beam shaping to form a Bessel function of the intensity. A glass slide mounted on a rotative stage is placed before the module whose edge is centered on the beam. Since the beam is passing through simultaneously in air and glass, two spots are formed and generate cracks oriented according to the writing direction as shown by Mishchik et al., 2017.

The sample is moved under the glass module thanks to axes in X and Y directions. The Z axis is used to position the Bessel beam in relation to the workpiece. The axes are controlled by the Aerotech software. A G code is generated to control the trajectories. The orientation of the rotary motion of the glass plate is synchronized with the movement of the X and Y axes, enabling to orient cracks according to the trajectory.

2.2. Different burst modes

The laser is able to produce a single pulse or a burst of pulses at a given frequency. The burst mode consists of generating several pulses in a raw. The delay between every pulse is of 25 ns. Two modes are achievable with the Yuja laser:

- The burst mode: in this case, the maximum energy (100 µJ) in a burst is divided according to the number of pulses as shown in the Fig 2 on the left. Note that energy repartition is not perfectly equally distributed but the sum of the energy per pulse is equal to the total energy per burst (here 100 µJ).
- The super burst mode: in this case, the maximum energy is contained in the first pulse (here 100 µJ), and the other pulses contain a decreasing energy as shown in the Fig 2 in the right. This allows to have more than 100 µJ per burst, for example to have up to 400 µJ per burst with 10 pulses at 22 kHz.

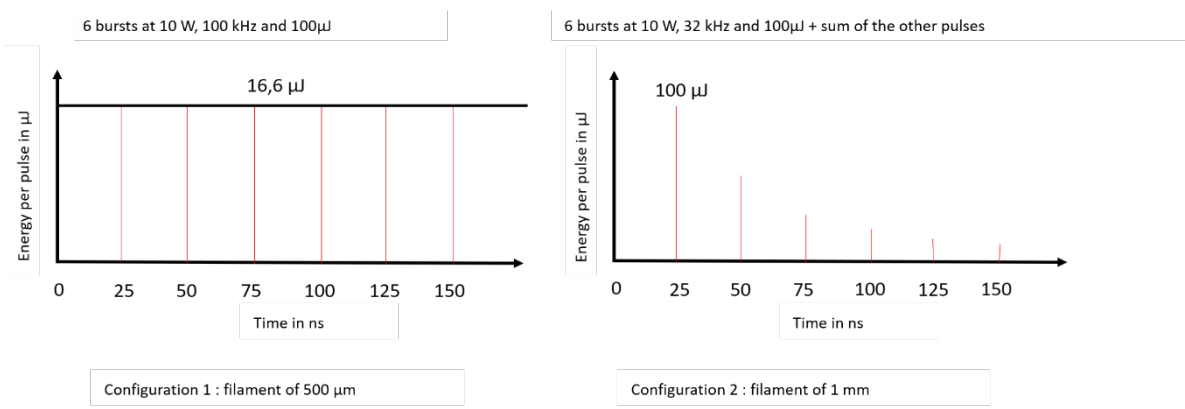

Fig. 2. Two different burst modes for energy accumulation.

The size of the beam before the module defines the length of the Bessel beam. The energy defines the length of the laser affected zone. In the first configuration the beam is expanded to reach a diameter of 7 mm before the module. In this case the filament is created by a single pulse or by a burst mode and the length reaches 500 µm at a maximum energy of 88 µJ. In the second configuration the size of the beam is about 4 mm. The beam is not expanded and the super burst mode is used. In this case the filament reaches a length of 1 mm with a maximum energy of about 400 µJ per burst with 10 pulses.

In the Fig 3, picture taken with an optical microscope illustrates the difference of glass cutting with the burst mode and the super burst mode.

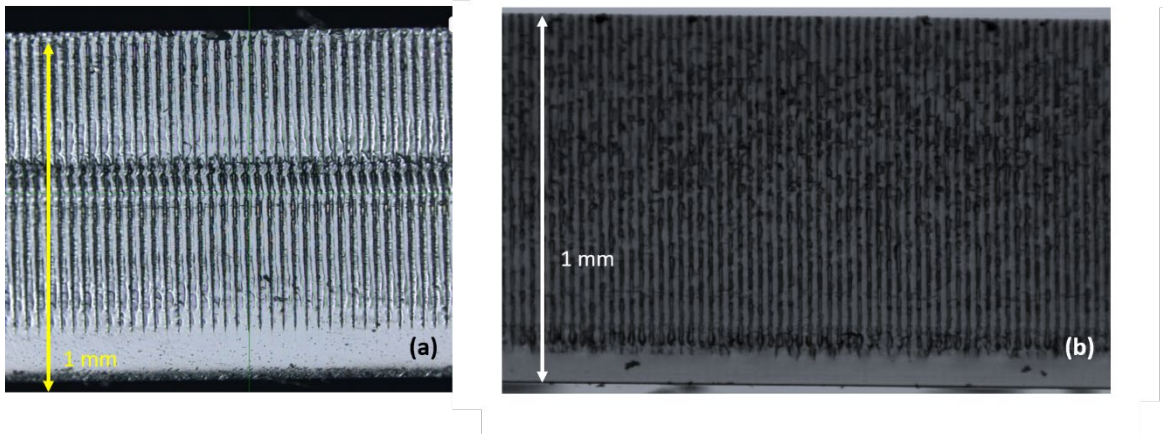

Fig. 3. Effect of the modes on the filament in glass. On the left (a) the burst mode with filament of 500 µm and two passes at two different positions in z. On the right (b) the super burst mode with filament of 1 mm and one pass.

On the left the burst mode is used with a filament of 500 µm therefore two passes are required to cut the entire thickness (1 mm) by changing the Z position between each pass. In addition, one filament contains 88 µJ maximum. On the right the super burst mode is used and allows to cut the glass with one pass and an energy of 400 µJ at 22 kHz. This configuration reduces by a factor 2 the cycle time.

3. Laser cutting

The goal of this part is to define the best parameters to reach a roughness smaller than 1 µm after cleaving along a line and curved shapes.

3.1. Effect of the energy deposition (burst mode)

It is known that the energy deposition plays a role on the induced stress (Champion et al.,2012, Champion et al. 2013). As cracks are created and oriented, we study the residual stress in the laser affected zones and the aspect of the lines inscribed with the laser. To do so, lines are made on the surface of the glass sample and the speed is varied from 50 mm/s to 500 mm/s at 88 µJ per burst and a frequency of 10 kHz. For this experiment trajectories are linear. The burst contains 5 pulses. In the graph on the Fig 4, pictures taken with a microscope in transmission illustrate the aspect of the lines. In addition, gray levels measured on the images taken with crossed polarized light correspond to the stress levels. These gray levels are plotted according to the energy deposition.

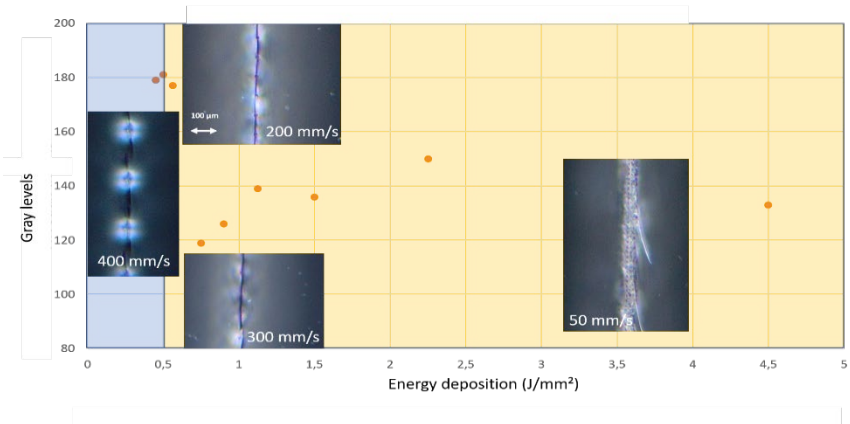

Fig. 4. Stress according to the energy deposition at 10 kHz.

At low energy deposition a build-up of stress is observed between cracks up to a maximum stress corresponding to the blue part on the graph. In these conditions, cracks form with a certain spacing and stress accumulates in between. Therefore, the cutting along the line is inhomogeneous and cleavage doesn't follow lines. When the energy deposition increases, the space between crack disappears (yellow part on the graph), and the stress relaxes along the entire line. In this case the cleavage is easier and with a better quality. If the energy deposition continues to rise, cracks disorganize and the quality of the cleavage decreases. Indeed, melted areas could form between filaments and weld locally the glass. According to these results, a speed between 200 mm/s and 300 mm/s is required to reach the best quality after cleaving.

As seen previously, the super burst mode allows to create filaments of 1 mm long with a beam of 4mm wide before the module. Therefore, the beam expander is removed from the optical path to create longer filaments. In addition, low frequency and the optimal speed allows to reduce the melted area along and between the filaments. Therefore, the optimal parameters to cut along a line are 10 pulses in a super burst, 10 kHz and a speed between 200 and 300 mm/s.

3.2. Cutting of different shapes

To achieve curved cut, an optical plate is rotated and synchronized with the translation axes so that the orientation of the created cracks can be controlled according to the cutting direction. The maximum speed with the synchronization is limited to 30 mm/s with the current hardware. Therefore, the frequency used to cut the curved shape is 1 kHz to keep the same distance between consecutive bursts. Regarding the tube, a motor rotates the tube with a chosen speed to perform the cutting.

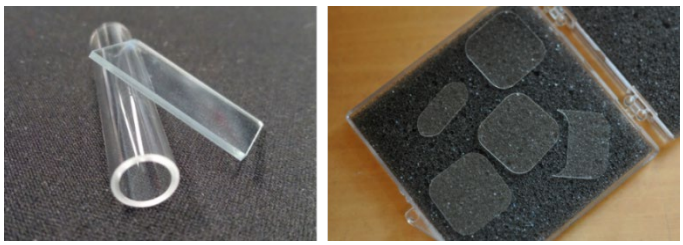

Fig. 5. Example of different shapes achievable.

In Fig 5, photos on the left, taken with a camera illustrate the transversal cut of a tube and a plate. On the right, squares of 10 mm with curved corners are shown. The cleavage gives a roughness smaller than 1 µm. Note that for small curve, the cleavage doesn't follow the trajectories therefore complex shapes cannot be achieved.

4. Laser welding applied to micro-fluidic

The goal of this part is to weld micro channels. Since Borofloat® plates are widely used in microfluidic due to its properties, plates of 1mm thick are used for the welding. Channels are inscribed on the surface of a plate by ablation and another plate is placed on the top to be welded with the module.

As seen previously, low frequency combined with the proper speed avoids heat accumulation. In addition, the super burst mode which can provide a burst energy of up to 400 µJ, enables to increase the size of the filament in the material. Under these conditions, cutting is achievable. Regarding the welding, we need to accumulate the heat to melt locally. To do so, the frequency is increased to reduce the distance between bursts and the number of pulses in one burst is studied for both modes exposed previously.

4.1. Effect of the number of pulses per burst

In this part we compare the residual stress in the laser affected zones according to the burst mode and the super burst mode for different number of pulses. Two plates made of Borofloat® are taken under the pressure to be closed to the optical contact and the laser is focused between plates to weld. Lines are made in a raw and spaced by 1 mm, moving the sample at 15 mm/s and changing the burst type for different numbers of pulses in the burst.

In the graph of the Fig 6, pictures taken with an optical microscope with crossed polarized light illustrate the welded channels. Gray levels are measured along the cross section of each line and normalized to compare measurements. These gray levels correspond to the stress levels. The normalized gray levels are plotted according to the number of pulses inside one burst. On the left the results for the burst mode and on the right the results for the super burst mode are shown.

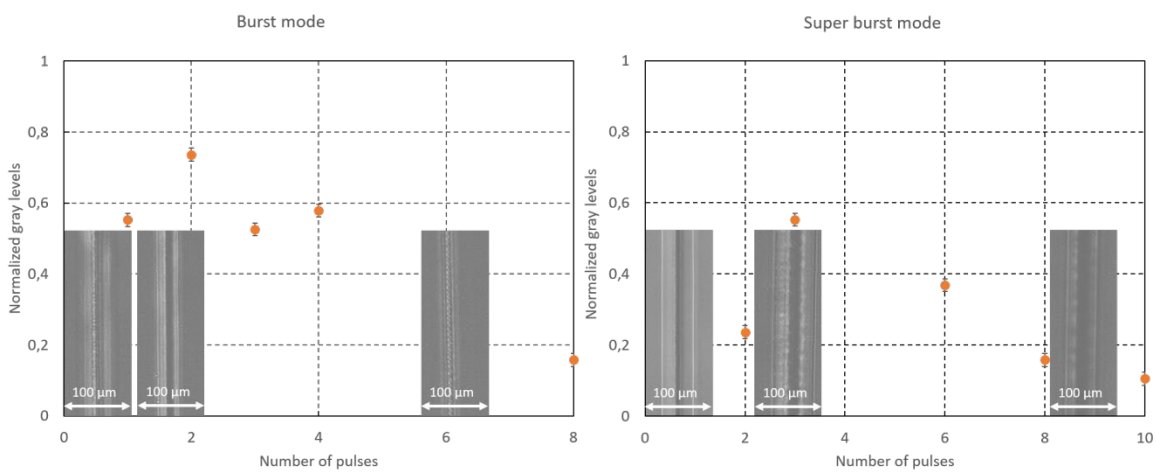

Fig. 6. Normalized gray levels according to the number of pulses per burst. On the left for the burst mode, on the right for the super burst mode.

In the graph on the left, with the burst mode, the stress reaches a peak when the number of pulses per burst increases up to 2. Then if the number of pulses increases, stress decreases and inhomogeneities are observed in the melted area. The energy per burst in this case stays constant at 50 µJ. The results show an increase on the heat accumulation with up to 2 pulses per burst. On the other hand, since the energy per pulse decreases with the number of pulses in the burst, the heat accumulation could stop after 3 pulses and the melted area decreases and the welding could not occur anymore. This could explain the decreasing of the stress and the partial melted areas (see the last picture of the graph).

In the graph on the right, with the super burst mode, the stress reaches a peak when the number of pulses per burst increases up to 3. Then if the number of pulses rises, stress decreases and inhomogeneities are observed in the melted area. In increasing the number of pulses, we increase the energy per burst as well from about 85 µJ to 227 µJ for 2 pulses and 10 pulses respectively. As seen previously, a heat accumulation takes place according to the number of pulses per burst. In the case of the super burst mode this accumulation doesn't stop and therefore, cracks could partially take place after 3 pulses and cause the inhomogeneities (cracks) and stress relaxation.

The burst mode gives a welding less homogeneous than the super burst mode as seen on the Fig 6. In addition, two pulses inside one burst seems to be the compromise in terms of heat accumulation.

4.2. Effect of the energy deposition

In the part of this work we use the following parameters: super burst mode, two pulses, 85 µJ, 59 kHz. Since we have defined the number of pulses in the super burst, we optimize the welding area in varying the energy deposition and study the stress and the aspect of the welded lines. The goal is to optimize the cycle time and the homogeneity of lines. Lines are melted as seen previously in varying the speed from 15 mm/s to 100 mm/s. In the graph of the Fig 7, the normalized gray levels corresponding to the stress, are plotted according to the energy deposition. Images taken with an optical microscope in transmission with crossed polarized light illustrate the aspect of the welding.

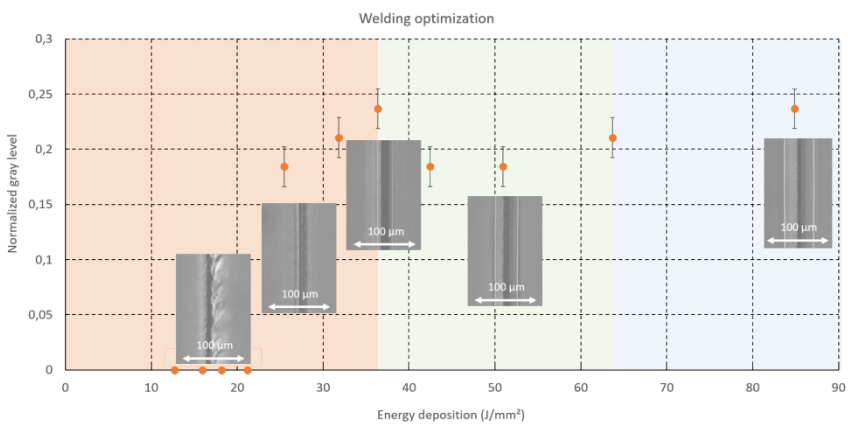

Fig. 7. Normalized gray levels according to the energy deposition.

At low energy deposition, welding doesn't take place. When the energy deposition increases, the glass starts to partially melt and the stress reaches a maximum (orange part in the graph) when the melting becomes homogeneous. As the energy deposition increases, the stress starts to increase again (green part of the graph) and the melted parts are bigger. Then the stress keeps rising (blue part on the graph) when the

energy deposition increases. The green part represents a compromise between a homogeneous melting and the stress accumulation. Therefore, we use a speed of 25 mm/s corresponding to 51 J/mm² to weld the channels as shown in continuation.

4.3. Welding of channels

Channels of 200 µm wide and 100 µm depth are made in a Borofloat® plate with a laser and a lens combined to a scanner head. The sample is cleaned in ultrasound bath. A second plate is put under pressure to reach the optical contact. Then the channels are welded with the defined parameters. In the Fig 8, on the left an image taken with a camera illustrates the welding.

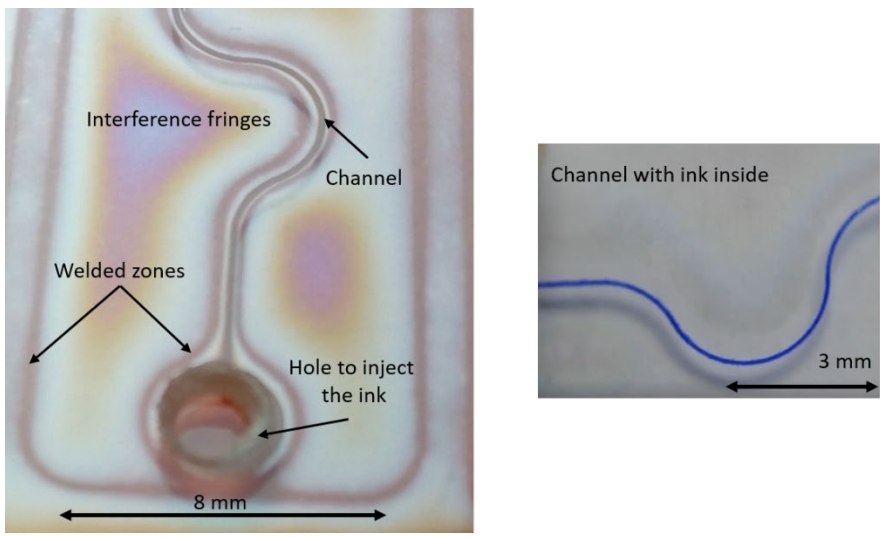

Fig. 8. Example of welding around a channel.

The welded zones surround the channel as shown in Fig 8 on the left. The interference fringes show that the optical contact is reached. Indeed, the color range appears from the dark gray, corresponding to the optical contact, to the blue. This means that the maximum distance between both plates after welding is about 300 nm. Then ink is injected with a syringe in the hole showed on the left. On the right an image of a channel with ink inside shows that there is no leakage. With this method long part can be welded thanks to the elongated melted zone using Bessel beam and the process is less sensitive to the eventual tilts. In addition, melted areas are more uniform than with a lens combined with a scanner head and the process is less sensitive to cracks formation along long path. Note that the repeatability and more complex shapes need to be check to make the process more industrial.

5. Conclusion

Glass cutting has been proven along a line and curved trajectories with a roughness smaller than 1 µm. The super burst is used to increase the energy and the length of the filament at low frequency to avoid melting between consecutive filaments. Different thicknesses are achievable from 200 µm up to 1 mm. Note

that the separation is done with a cleavage. Complex forms, with small radius curvature are not possible with cleavage. Indeed, a local heat is necessary to separate the pieces of glass.

A good control of the heat accumulation has been shown allowing to weld locally long channels of few millimeters using the super burst and high frequency regime (59 kHz).

The super burst mode is used to accumulate and increase the energy per burst. To cut the glass, low frequency and high energy is required using the super burst whereas in order to melt, high frequency and less energy per super burst allows to accumulate the heat and locally melt the glass avoiding cracks. Regarding the welding, more complex shape and repeatability need to be tested.

These results demonstrate the possibility to perform both operations, cutting and welding, by using a single laser system which can be of huge interest for application or production in the field of microfluidics.

References

Canning, J., Lancry, M., Cook, K., Weickman, A., Brisset, F., and Poumellec, B., 2011. Anatomy of a femtosecond laser processed silica waveguide [Invited], Optical Materials Express 1, p.998–1008.

Davis, K. M., Miura, K., Sugimoto, N., and Hirao, K., 1996. Writing waveguides in glass with a femtosecond laser, Optics. Letters. 21, p. 1729–1731.

Champion, A. and Bellouard, Y., 2012. Direct volume variation measurements in fused silica specimens exposed to femtosecond laser, Optical Materials Express 2, p. 789-798.

Champion, A., Beresna, M., Kazansky, P., and Bellouard, Y., 2013. Stress distribution around femtosecond laser affected zones: effect of nanogratings orientation, Optics Express 21, p. 24942–24951.

Fibich, G. and Gaeta, A. L., 2000. Critical power for self-focusing in bulk media and in hollow waveguides, Optics. Letters. 25, p. 335.

Mourou, G. A. et al. 2006, Optics in the relativistic regime, Reviews of Modern. Physics. 78, p. 309.

Couairon, A. and Bergé, L., 2000. Modeling the filamentation of ultra-short pulses in ionizing media, Physics of Plasmas 7, p. 193.

Kumkar, M., Kaiser, M., Kleiner, J., Grossmann, D., Flamm, D., Bergner, K., Nolte, S., 2014. Cutting of Transparent Materials by Tailored Absorption, in Advanced Solid State Lasers, OSA Technical Digest (online), paper ATh1A.2.

Mishchik, K., Beuton, R., Caulier, O. D., Skupin, S., Chimier, B. Duchateau, G., Chassagne, B., Kling, R., Honninger, C., Mottay, E., Lopez, J., 2017. Improved laser glass cutting by spatio-temporal control of energy deposition using bursts of femtosecond pulses, Optical Society of America under the terms of the OSA Open Access Publishing Agreement, Laser materials processing, p. 140–3390, Femtosecond phenomena, p. 320–2250, Glass and other amorphous materials, p. 160–2750.

Kongsuwan, P., Satoh, G., Lawrence Yao, 2012. Transmission Welding of Glass by Femtosecond Laser: Mechanism and Fracture Strength, Journal of Manufacturing Science and Engineering, 134, p. 011004.